Photonic crystal nanofishbone nanocavity

Tsan-Wen Lu and Po-Tsung Lee*

Department of Photonics and Institute of Electro-Optical Engineering, National Chiao Tung University, Rm. 413 CPT Building, 1001 Ta-Hsueh Road, Hsinchu 30010, Taiwan

**Corresponding author: potsung@mail.nctu.edu.tw*

Received May 9, 2013; revised July 15, 2013; accepted July 19, 2013; posted July 22, 2013 (Doc. ID 190322); published August 14, 2013

We propose a photonic crystal (PhC) nanofishbone (NFB) nanocavity, which confines an ultrahigh Q ($\sim 1.8 \times 10^7$) transverse-magnetic (TM) mode. With thin slab thickness and only few PhC periods, the TM mode in NFB nanocavity shows higher Q, larger confinement factor and smaller mode volume than that in PhC nanobeam nanocavity, while the total etched-surface area is also significantly reduced. This PhC NFB nanocavity with very compact device size will be very beneficial for quantum cascade lasers, plasmonic nanolasers, and other applications needing high Q TM modes.

OCIS codes: (230.5298) Photonic crystals; (140.3945) Microcavities; (230.5750) Resonators.
http://dx.doi.org/10.1364/OL.38.003129

In the last decade, various two-dimensional (2D) transverse-electric (TE)-polarized photonic crystal (PhC) nanocavities have been widely studied, whose 2D PhCs are usually formed by air holes on dielectric slabs. Owing to their ultrahigh quality factors (Qs) and ultrasmall mode volumes (Vs), this kind of nanocavity had obtained tremendous successes in nanolasers [1], optical sensors [2], and other functional passive components [3,4]. Although transverse-magnetic (TM)-polarized PhC nanocavities draw less attention on the roadmap, they are still very important in various applications, especially for quantum cascade lasers (QCLs) [5,6], silicon lasers with horizontal gain slots [7,8], plasmonic nanolasers [9], and so on. However, unlike TE-polarized PhC nanocavities constructed on dielectric slabs, TM-polarized PhC nanocavities are usually designed via 2D dielectric rods for large TM-polarized photonic band-gap, which has several significant drawbacks. First, using 2D dielectric rods to form a PhC nanocavity results in large device footprint. Second, the structural discontinuity of dielectric rods makes current injection difficult when serving as an active light source. Third, the claddings and substrates with refractive indices larger than air are the essentials for supporting the discontinuous rods, which limit Qs of the nanocavities.

In recent years, the successes of 2D PhC nanocavities have been evolved to one-dimensional (1D) PhC system on nanobeams (NBs) [10–13]. And Zhang *et al.* further propose that a high Q ($\sim 2.4 \times 10^6$) TM_{00} mode can be confined in a 1D PhC nanocavity on suspended NB [14]. This TM-polarized 1D PhC NB nanocavity with structural continuity can simultaneously overcome the drawbacks of large device footprint, difficulty of current injection, and low Q in 2D TM-polarized PhC nanocavity based on dielectric rods. In this report, we propose a different design named PhC nanofishbone (NFB) nanocavity with TM_{10} mode. With thin slab thickness and only few PhC periods, the TM_{10} mode in NFB nanocavity shows higher Q, larger confinement factor, and smaller mode volume than those of TM_{00} mode in NB nanocavity, while the total etched-surface area of NFB nanocavity is also significantly reduced.

Scheme of 1D PhC NFB is shown in Fig. 1(a). Unlike 1D PhC NB with periodic air-holes located at the center of ridge waveguide, 1D PhC NFB consists of periodic half air-holes on both sides of the ridge waveguide. The parameters of 1D PhC NFB, including lattice constant a, half air-hole radius r, NFB width w, and thickness t_{NFB}, are defined in Fig. 1(a). With $w = a$, $r/a = 0.34$, $t_{NFB} = a$, and refractive index (n_{Si}) of 3.46 for silicon (Si), theoretic TM-like band diagram of 1D PhC NFB is performed by plane wave expansion (PWE) method and shown in Fig. 1(b). Theoretic E_z fields of the first three bands at $k_x = 0.5(2\pi/a)$ are shown in Fig. 1(c). In our studies, instead of using the fundamental TM_{00} modes (first and second bands), we will focus on the odd-like TM_{10} mode (third band) with field concentrated in the regions between the half air-holes.

To well confine the TM_{10} mode at $k_x = 0.5(2\pi/a)$, we design a 1D PhC NFB nanocavity with the outer and tapered mirrors on both sides as illustrated in Fig. 2(a) according to the principle of Bloch mode index matching [15]. The outer mirror is a five-period PhC with fixed a, and the tapered mirror is formed by a eight-period gradually varied PhC, whose lattice constant $a_n = (1 - 0.02n)a (n = 1–8)$ with fixed half air-hole radius (r_n) over $a_n(r_n/a_n)$ ratio of 0.34. Therefore, total PhC period number P on each side of the nanocavity is 13.

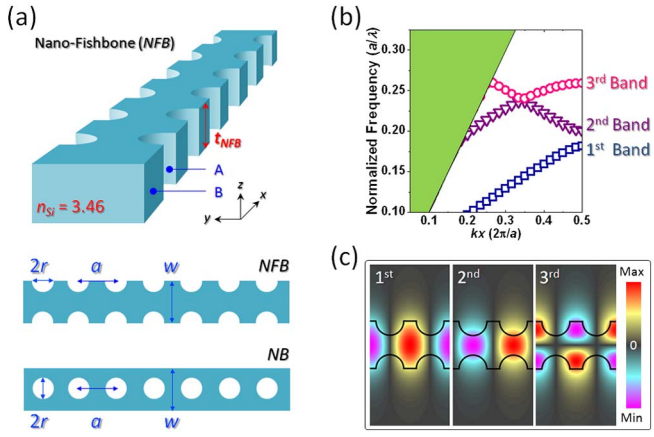

Fig. 1. (a) Schemes and lattice parameters of 1D PhC NFB and NB. (b) The first three TM-like bands in 1D PhC NFB and (c) their theoretic mode profiles in E_z fields at $k_x = 0.5(2\pi/a)$ via PWE method.

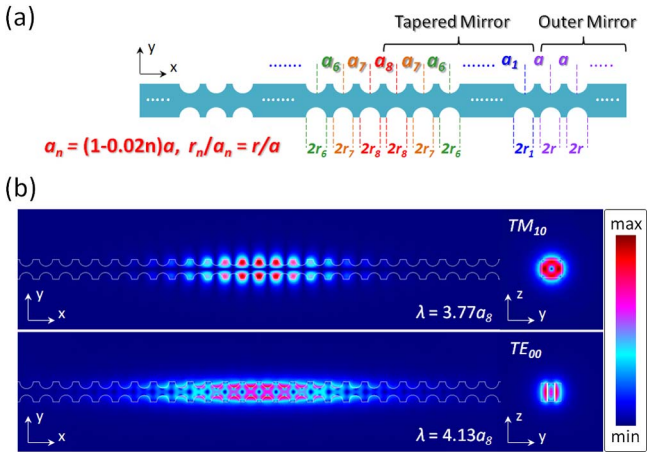

Fig. 2. (a) Design of 1D PhC NFB nanocavity with the tapered and outer mirrors. (b) Theoretic mode profiles at x–y and y–z planes of (top) TM_{10} (in $|E_z|$ fields) and (bottom) TE_{00} (in $|E_t|$ fields) modes confined in 1D PhC NFB nanocavity.

With n_{Si}, t_{NFB}, and w of 3.46, $0.90a$, and a, the simulated TM_{10} mode profiles in $|E_z|$ fields at x–y and y–z planes in 1D PhC NFB nanocavity via three-dimensional (3D) finite-element method (FEM) are shown in Fig. 2(b), which has ultrahigh Q of 1.8×10^7 and small V of $1.14(\lambda/n_{Si})^3$. Furthermore, this nanocavity also confines a TE_{00} mode but with low Q of 3.9×10^4, which is beneficial for applications only needing TM mode. The simulated TE_{00} mode profiles in $|E_t| = |(E_x^2 + E_y^2)^{1/2}|$ fields at x–y and y–z planes are shown in Fig. 2(b).

We then investigate the dependences of Q on P, t_{NFB}, w, and r/a. In Fig. 3(a), with fixed $w = a$, $r/a = 0.34$, and $t_{NFB} = 0.90a$, Q decreases with reducing P owing to the weakened optical confinements by the decreased PhC mirror periods. However, Q is still close to 10^6 when $P = 10$. We should note that $P = 8$ in Fig. 3(a) means 1D PhC NFB nanocavity only has an eight-period tapered mirror and $P = 6$ means a six-period tapered mirror with lattices from a_3 to a_8. In Fig. 3(b), with fixed $w = a$, $r/a = 0.34$, and $P = 13$, Q is larger than 10^7 in the range of $t_{NFB} = 0.60a$–$1.10a$. When $t_{NFB} < 0.6a$, Q decreases because of the cutoff thickness of fundamental TM mode. And Q decreases when $t_{NFB} > 1.1a$. This is because the mode frequency becomes lower when t_{NFB} increases and the lattice modulation of NFB nanocavity becomes gentle, which leads to reduced mode gap and thus results in weakened confinement and decreased Q [16]. In Fig. 3(c), with fixed $P = 13$ and $t_{NFB} = 0.90a$, Q is always larger than 10^6 in our studied ranges of $w = 0.85a$–$1.03a$ and $r/a = 0.29$–0.36, which shows very large fabrication tolerances of 1D PhC NFB nanocavity. We also consider the fabrication imperfection of linearly increased r_n/a_n ratio from the outer mirror to nanocavity caused by proximity effect during electron-beam lithography. With fixed r/a of 0.34, Q of TM_{10} mode in NFB nanocavity degrades when $\Delta r/a$ (defined as r_8/a_8–r/a) increases, but is still higher than 4×10^6 when $\Delta r/a$ is 0.02, which shows large fabrication tolerance again. In addition, the dependence of confinement factor γ_d (defined as the ratio of mode energy concentrated in dielectric region) on t_{NFB} is shown in Fig. 3(b). γ_d factor is always larger than 0.5 within a large range of $t_{NFB}(0.60a$–$1.80a)$, which means strong light–matter interactions by TM_{10} mode in 1D PhC NFB nanocavity for serving as active light emitters.

Furthermore, we investigate the dependences of Q on P, w, r/a, and t_{NFB} when 1D PhC NFB nanocavity is made of low index materials, for example, silicon carbide (SiC) with refractive index (n_{SiC}) of 2.6. In Figs. 3(a) and 3(b), Q is larger than 10^5 when $P > 10$ (with fixed $t_{NFB} = 0.90a$) or $t_{NFB} = 0.70a$–$1.45a$ (with fixed $P = 13$), which is sufficient for most applications needing high Qs. In Fig. 3(d), with fixed $P = 13$ and $t_{NFB} = 0.90a$, Q is larger than 10^5 in our studied ranges of $w = 0.91a$–$1.06a$ and $r/a = 0.29$–0.36. With P, t_{NFB}, r/a, and w of 13, $0.90a$, 0.34, and $1.06a$, the TM_{10} mode shows higher Q of 1.1×10^6 and smaller V of $0.42(\lambda/n_{SiC})^3$ than those of TE-polarized 2D PhC nanocavity on SiC slab [17]. Therefore, we can conclude that our proposed 1D PhC NFB nanocavity still shows good TM mode properties and large design tolerances even being applied to a low index material system.

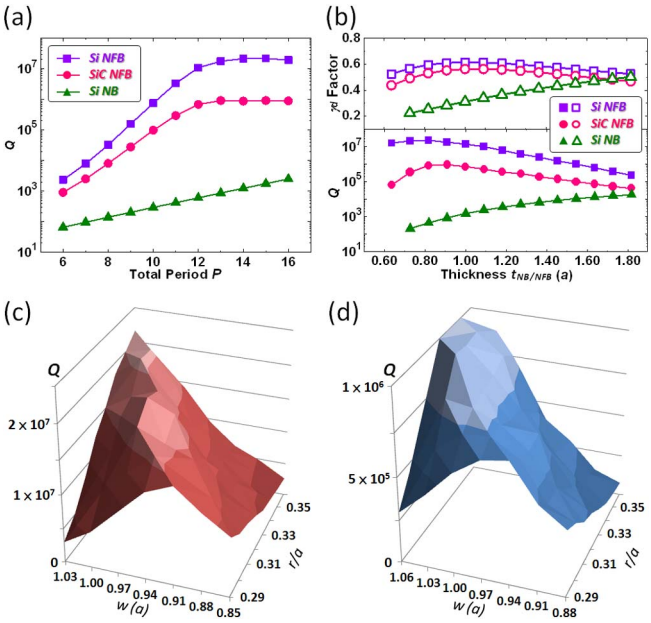

Fig. 3. Theoretic Q and γ_d factors of the TM_{10} modes in 1D PhC Si, SiC NFB nanocavities, and the TM_{00} modes in 1D PhC Si NB nanocavities as functions of (a) P and (b) t_{NFB}. Theoretic Q mappings of the TM_{10} modes in 1D PhC (c) Si and (d) SiC NFB nanocavities as functions of w and r/a.

Under the premise of compact device sizes and with the parameters defined in Fig. 1(a), we simulate the previously studied low-loss TM_{00} mode in 1D PhC Si NB nanocavity by Zhang *et al.* [14]. With $w = a$, $r/a = 0.34$, NB thickness $t_{NB} = 0.90a$, $n_{Si} = 3.46$, and $P = 13$, the TM_{00} mode profiles in $|E_z|$ fields at x–y and y–z planes confined in 1D PhC NB nanocavity are shown in Fig. 4(a), which has much lower Q of 900 and larger V of $2.80(\lambda/n_{Si})^3$ than those of TM_{10} mode in 1D PhC NFB nanocavity. The differences in Q and V can be understood by the $|E_z|$ field cross-sectional distributions of the TM_{10} and TM_{00} modes in 1D PhC NFB and NB nanocavities shown in Fig. 4(b). The field distribution of TM_{10} mode in 1D PhC NFB nanocavity shows a Gaussian distribution with narrow line-width and strong

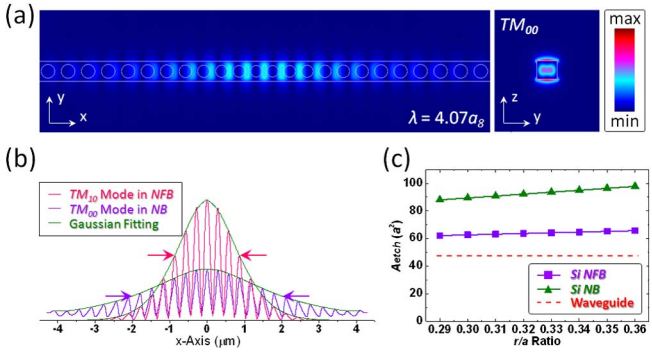

Fig. 4. (a) Theoretic TM_{00} mode profiles in $|E_z|$ fields at x–y and y–z planes in 1D PhC NB nanocavity via 3D FEM. (b) Cross-sectional $|E_z|$ field distributions with Gaussian fittings of the TM_{10} and TM_{00} modes in 1D PhC NFB and NB nanocavities with the same parameters. (c) Theoretic A_{etch} of 1D PhC NFB and NB nanocavities as a function of r/a ratio from 0.29 to 0.36 with fixed P of 13.

field enhancement, which are responsible for small V and high Q of TM_{10} mode in 1D PhC NFB nanocavity with very few periods. However, for the TM_{00} mode in 1D PhC NB nanocavity, 13 PhC periods on each side of the nanocavity are insufficient to form a complete Gaussian distribution, thus leading to significant optical losses into the light cone and resulting in a relatively low Q and large V when the device size is too compact.

The dependences of Q on P and t_{NB} of TM_{00} mode in 1D PhC NB nanocavity with fixed r/a and w of 0.34 and a are shown in Figs. 3(a) and 3(b), which show lower values than those of 1D PhC Si and SiC NFB nanocavities and with different trends. Dissimilar with those of TM_{10} mode in 1D PhC Si and SiC NFB nanocavities, Q of TM_{00} mode in 1D PhC NB nanocavity increases with P and t_{NB} monotonically for the cases studied. One can obtain a high Q ($\sim 9.7 \times 10^6$) [8] TM_{00} mode with small V ($\sim 1.2(\lambda/n)^3$) via further increasing both P and t_{NB} to 22 and $3a$. However, the device size is relatively massive compared with NFB nanocavity with TM_{10} mode. Since the TM_{10} mode in NFB nanocavity can reach high Q under less P than the TM_{00} mode in NB nanocavity needs, via directly launching lightwave, the TM_{10} mode in NFB nanocavity with $P = 8$ shows narrower transmission bandwidth ($\sim$0.12 nm) than that ($\sim$10 nm) of TM_{00} mode in NB nanocavity with the same P, which is beneficial for compact-sized passive optical filters, splitters, and so on. Furthermore, with $P = 13$ and in the range of $t_{NFB} = 0.60a$–$1.80a$, γ_d factors of TM_{10} mode in SiN FB nanocavities are always larger than that ($\sim$0.5) of TM_{00} mode in Si NB nanocavity with $t_{NB} = 1.80a$, as shown in Fig. 3(b). Therefore, we can conclude that our proposed 1D PhC NFB nanocavity design shows great benefits for achieving ultrahigh Q and large γ_d factor in very compact sizes with large design tolerance.

Moreover, another important feature of 1D PhC NFB nanocavity is the reduced total-etched surface area A_{etch} [defined as area summation of the sidewalls A and B denoted in Fig. 1(a)]. In optoelectronic devices, nonradiative surface recombination increases with the surface area, especially the destructively etched surface. Therefore, minimization of the etched surface area can reduce unnecessary carrier losses, which is beneficial

Table 1. Comparisons of TM_{10} and TM_{00} Mode Properties in 1D PhC Si NFB and NB Nanocavities with Fixed $r/a = 0.34$, $w = a$, and Compact Device Size ($t_{NB} = t_{NFB} = 0.90a$, and $P = 13$)

	Q	V $((\lambda/n_{Si})^3)$	γ_d	λ	A_{etch}
NFB	1.8×10^7	1.14	0.61	$3.77a_8$	$64.7a^2$
NB	9.0×10^2	2.80	0.28	$4.07a_8$	$95.1a^2$

for active light emitters. With fixed $P = 13$, $t_{NB} = t_{NFB} = 0.90a$, and $w = a$, Fig. 4(c) shows A_{etch} of 1D PhC NFB and NB nanocavities as a function of r/a ratio from 0.29 to 0.36, where 1D PhC NFB nanocavities show 30%–33% reduction in A_{etch} compared with 1D PhC NB nanocavities. The dashed line in Fig. 4(c) represents the A_{etch} ($\sim 47.7a^2$) of a ridge waveguide with equal length for reference. Therefore, in addition to achieving high Q with very compact device size, our proposed 1D PhC NFB nanocavity also shows much reduced etched surface area.

In summary, we propose and theoretically investigate a TM-polarized 1D PhC NFB nanocavity. As summarized in Table 1, for compact device size ($t_{NFB} = 0.90a$, $w = a$, and $P = 13$), this design confines an ultrahigh Q ($\sim 1.8 \times 10^7$) TM_{10} mode with smaller mode volume V, smaller etched surface area A_{etch}, and higher γ_d factor than those of TM_{00} mode in NB nanocavities with the same parameters. We believe the presented 1D PhC NFB nanocavity with compact device size and continuous slab structure is very beneficial for QCLs, light emitters, plasmonic nanolasers, and other applications needing high Q TM modes.

This work is supported by Taiwan's National Science Council (NSC) under contract numbers NSC-100-2221-E-009-109-MY3 and NSC-101-2221-E-009-054-MY2. The authors would like to thank the help from Center for Nano Science and Technology (CNST) of National Chiao Tung University (NCTU), Taiwan.

References

1. B. Ellis, M. Mayer, G. Shambat, T. Sarmiento, E. Haller, J. S. Harris, and J. Vuckovic, Nat. Photonics **5**, 297 (2011).
2. S. Kita, S. Otsuka, S. Hachuda, T. Endo, Y. Imai, Y. Nishijima, H. Misawa, and T. Baba, Opt. Express **19**, 17683 (2011).
3. M. Barthaand and O. Benson, Appl. Phys. Lett. **89**, 253114 (2006).
4. K. Nozaki, A. Shinya, S. Matsuo, Y. Suzaki, T. Segawa, T. Sato, Y. Kawaguchi, R. Takahashi, and M. Notomi, Nat. Photonics **6**, 248 (2012).
5. Y. Chassagneux, R. Colombelli, W. Maineult, S. Barbieri, S. P. Khanna, E. H. Linfield, and A. G. Davies, Appl. Phys. Lett. **96**, 031104 (2010).
6. M. Bahriz, V. Moreau, R. Colombelli, O. Crisafulli, and O. Painter, Opt. Express **15**, 5948 (2007).
7. D. Mascoli, D. Gerace, and L. C. Andreani, Photon. Nanostruct. Fundam. Appl. **9**, 63 (2011).
8. T. W. Lu, P. T. Lin, and P. T. Lee, Opt. Lett. **37**, 569 (2012).
9. A. M. Lakhani, M. Kim, E. K. Lau, and M. C. Wu, Opt. Express **19**, 18237 (2011).
10. Y. Zhang, M. Khan, Y. Huang, J. H. Ryou, P. B. Deotare, R. Dupuis, and M. Lončar, Appl. Phys. Lett. **97**, 051104 (2010).
11. B. Wang, M. A. Dündar, R. Nötzel, F. Karouta, S. He, and R. W. van der Heijden, Appl. Phys. Lett. **97**, 151105 (2010).

12. Y. F. Chen, X. Serey, R. Sarkar, P. Chen, and D. Erickson, Nano Lett. **12**, 1633 (2012).
13. L. D. Haret, T. Tanabe, E. Kuramochi, and M. Notomi, Opt. Express **17**, 21108 (2009).
14. Y. Zhang, M. W. McCutcheon, I. B. Burgess, and M. Lončar, Opt. Lett. **34**, 2694 (2009).
15. P. B. Deotare, M. W. McCutcheon, I. W. Frank, M. Khan, and M. Lončar, Appl. Phys. Lett. **94**, 121106 (2009).
16. M. Notomi, E. Kuramochi, and H. Taniyama, Opt. Express **16**, 11095 (2008).
17. B. S. Song, S. Yamada, T. Asano, and S. Noda, Opt. Express **19**, 11084 (2011).